Internal Tides and Solitary Waves in the Northern South China Sea: A Nonhydrostatic Numerical Investigation

Ping-Tung Shaw
Dept of MEAS, North Carolina State University
Box 8208, Raleigh, NC 27695-8208
Phone: (919)515-7276 FAX: (919)515-7802 e-mail: pt_shaw@ncsu.edu

Shenn-Yu Chao
Horn Point Laboratory, UMCES
P. O. Box 775, Cambridge, MD 21613-0775
Phone: (410)221-8427 FAX: (410)221-8490 e-mail: chao@hpl.umces.edu

Award Number: N00014-05-1-0280 (NCSU)
Award Number: N00014-05-1-0279 (UMCES)

LONG-TERM GOALS

The goal of this project is to understand processes relevant to the generation, propagation and dissipation of finite-amplitude internal solitary waves observed in the region from the Luzon Strait to the Chinese continental shelf.

OBJECTIVES

With data available from field observations in Non-Linear Internal Wave Initiative (NLIWI), this project is to perform simulation of finite-amplitude internal solitary waves under scenarios in the northern South China Sea. The objective is to provide information on the characteristics of nonlinear internal waves for comparison with data collected from remote sensing, mooring measurements, and shipboard observations.

APPROACH

Processes of wave generation, propagation and dissipation are studied by numerical simulation using a nonhydrostatic ocean model under different scenarios of bottom topography and stratification. Experiments include wave generation by ridges in the Luzon Strait and by density fronts, wave propagation across the deep basin with a shoaling thermocline, wave reflection and diffraction near the Dongsha Island, wave generation and dissipation on the continental slope, and characteristics of higher-mode waves.

WORK COMPLETED

A main thrust last year was the study of the wave generation process over the ridge in the Luzon Strait. Using a nonhydrostatic model (Shaw and Chao, 2006), we have systematically analyzed the dependence of wave generation on the ridge slope, stratification and the strength of the tidal currents. A manuscript (Shaw et al, 2008) has finished the first round of review and is under revision.

RESULTS

The experiments examine the effects of ridge width, barotropic tidal strength, and stratification on wave generation. Tidal forcing is included by specifying the sinusoidal barotropic inflow/outflow velocity on the two x-boundaries. The tidal current starts from zero at $t = 0$ as an ebb tide with eastward flow. In most experiments, the maximum tidal velocity on open boundaries (u_0) is 0.1 m/s. Although the semidiurnal tides are used in all experiments to facilitate discussion, similar conclusions can be extended to diurnal tides. All experiments use a time step of 31.05 s, which is 1/120 of the semidiurnal tidal period (12.42 hours). All experiments run for five tidal cycles.

The main finding is that the process of solitary wave generation consists of two steps. In the first step, barotropic tidal flow produces vertically propagating internal waves in the form of slanting wave beams emitting from the ridge top. In the second step, wave reflection and refraction traps internal wave energy along the thermocline, producing horizontally-propagating internal tides. If the amplitude of the internal tides is large, nonlinear steepening produces internal solitary waves. The process is described in details below.

1) Production of internal wave beams

The numerical experiments demonstrate the generation of internal wave beams over the ridge top by an oscillating tidal current as described in linear internal wave theory even though the ridge is tall and the flow is strongly nonlinear. Internal waves are produced when the slope of the ridge is steeper than that of the internal wave beam. Linear wave theory shows that the slope of the wave beam in an ocean with constant buoyancy frequency (N_0) is $\tan\phi = \sqrt{\left(\omega^2 - f^2\right)/\left(N_0^2 - \omega^2\right)}$, where ϕ is the angle between the wave beam and the horizontal axis, ω is the wave frequency, and f is the Coriolis parameter. Thus, internal wave generation depends on stratification at the ridge top and the frequency of the tidal currents. As the buoyancy frequency increases and the tidal period increases, wave beams become more horizontal, allowing generation of internal tides over a less steep ridge.

Figure 1 shows contour plots of the u-velocity at the end of the third tidal cycle (t = 37.26 hours) for ridges with different half widths (L). Note the existence of internal wave beams on the ridge and the evolution of vertically propagating internal waves into first-mode shallow-water waves because of wave reflection and refraction. In Figure 1a, the wave beam is steep and energy in the wave beam is high. The first-mode waves intensify to become internal solitary waves at about 100 km away from the ridge. As the ridge slope decreases, energy in the wave beam decreases but internal solitary waves still form in Figure 1b. When the ridge half width increases to 45 km (Figure 1c), internal wave energy emits from the ridge along a less steep slope and is much weaker. The flow field resembles that of a linear wave at $x = -100$ km and is quickly dissipated by $x = -170$ km (Figure 1c). Little internal wave energy leaves the ridge when L is further increased to 60 km (Figure 1d). In linear theory, the slope of the internal wave beams must exceed the ridge slope for internal wave generation. This statement still holds here when a ridge is of large amplitude and the flow is nonlinear. The gentle ridge in Figure 1(c) and (d) suppresses the generation of internal waves. Thus, one criterion for the generation of internal tides is that the ridge slope exceeds the slope of the wave beam at the tidal periods. When this is the case, enough energy is converted from the barotropic tide to the baroclinic tide to form solitary waves.

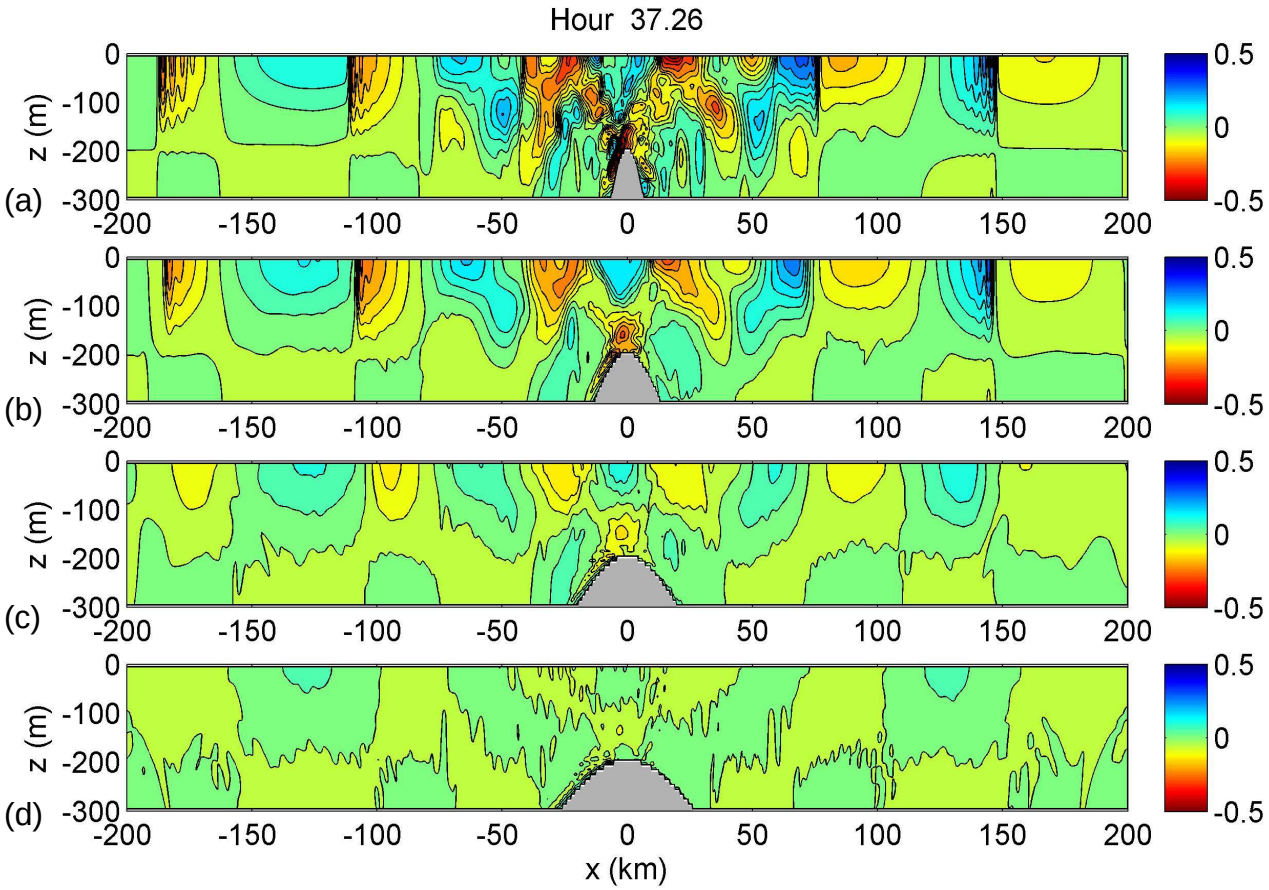

Figure 1 Contour plots of u velocity at slack water before flood tide at t = 37.26 hours for different half widths of the ridge (L): (a) 15 km, (b) 30 km, (c) 45 km, and (d) 60 km. The

If the barotropic velocity is doubled to 0.2 m/s, sharp fronts form in the experiment for L = 45 km (Figure 2). However, for L = 60 km, still little barotropic energy is converted to internal wave energy. A stronger tidal current increases the strength of the internal waves when the ridge slope is near critical, but has little effect on wave generation when the ridge slope is much less than the critical value. In Figure 3, the buoyancy frequency is reduced by half throughout the water column. Strong internal waves are generated for L = 15 km. Increasing L to 30 km significantly reduces the strength of the internal waves. Note that at L = 30 km, strong internal solitary waves are generated in the case of a stronger stratification in Figure 1b. Decreasing the stratification increases the slope of the wave beam, requiring a steeper ridge slope for wave generation.

2) Focusing of energy by a thermocline

Development of internal solitary waves involves not only the conversion of barotropic tidal energy to baroclinic waves but also the formation of horizontally propagating internal waves at the thermocline [Gerkema, 2001; Akylas et al., 2007]. Thus, generation of internal solitary waves is a two-step process. First, internal wave beams are produced by the barotropic tides over a ridge. This step requires a supercritical ridge slope. In the second step, a sharp thermocline is needed to trap the energy in the wave beam.

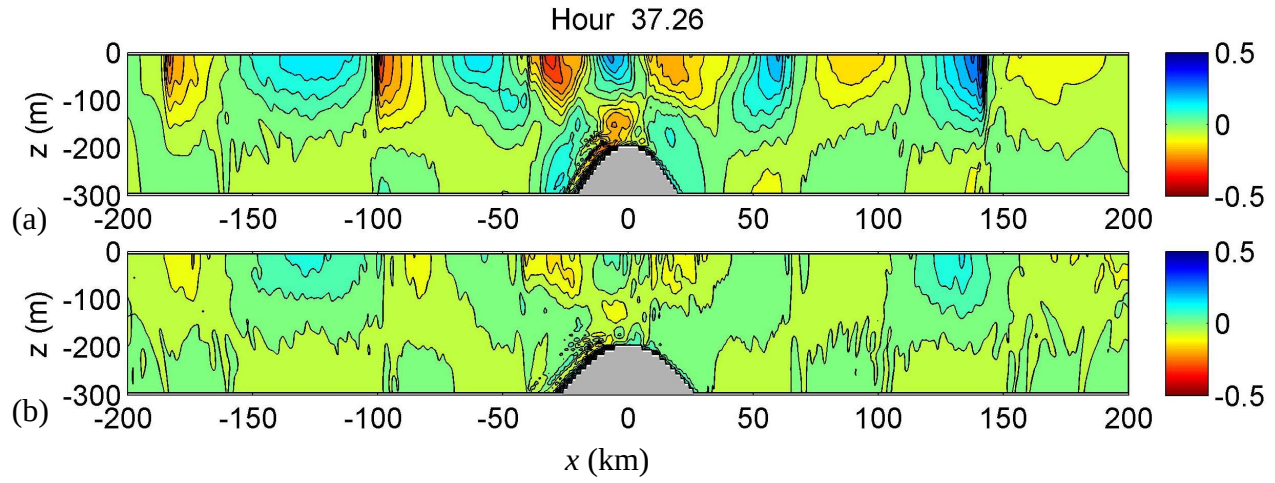

Figure 2 Contour plots of u velocity at slack water before flood tide at t = 37.26 hours. The parameters are the same as in Figure 1 except doubling the amplitude of the tidal current: (a) L = 45 km and (b) L = 60 km. The contour interval is 0.05 m/s.

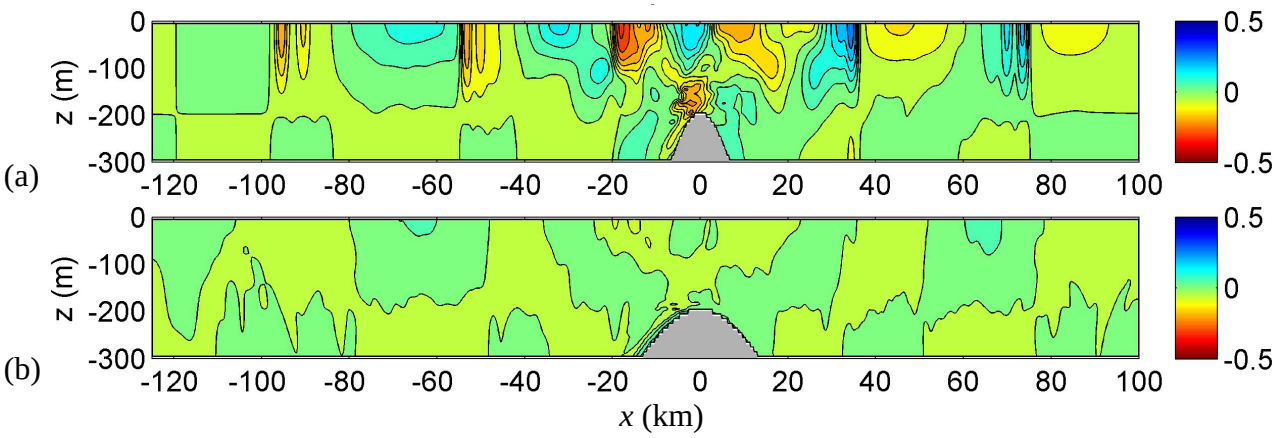

Figure 3 Contour plots of u velocity at slack water before flood tide at t = 37.26 hours. The parameters are the same as in Figure 1 except the buoyancy frequency is reduced by half: (a) L = 15 km and (b) L = 30 km. The contour interval is 0.05 m/s.

The next set of experiments uses the same parameters as those for a ridge of half width 30 km in Figure 1b but the upper ocean now contains a mixed layer 50 and 150 m deep, respectively (Figure 4a and 4b). The mixed layer is weakly stratified with a buoyancy frequency of 2×10^{-4} rad/s, allowing internal waves at the semi-diurnal frequency to propagate in the mixed layer. In Figure 4a, solitary wave trains appear in the *u*-velocity field at hour 37.26; development of internal solitary waves is not affected by the presence of a shallow mixed layer. If the mixed layer depth increases to 150 m, it effectively erases the thermocline at 100 m. Internal wave propagation is hardly seen (Figure 4b). Another experiment has been conducted to further distinguish the role of the thermocline in internal

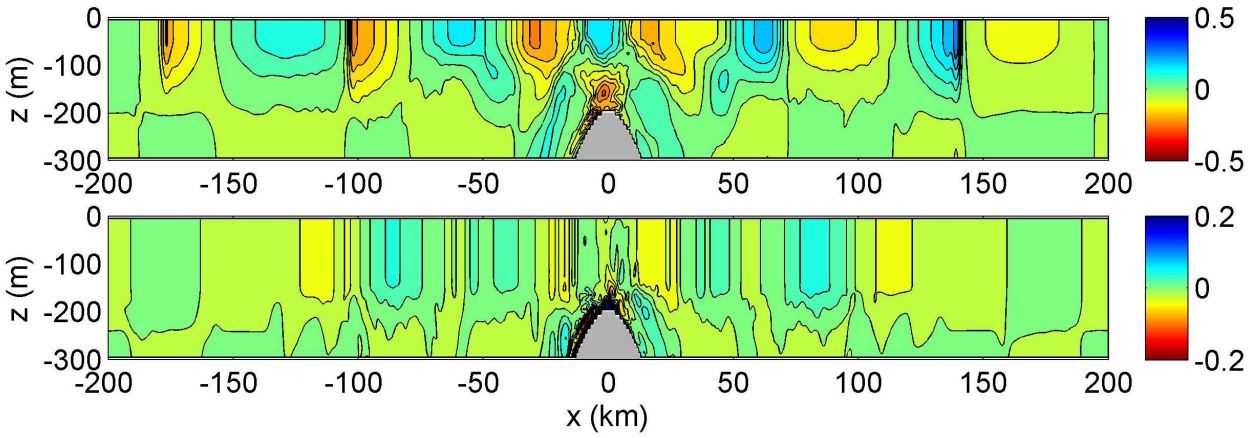

Figure 4 Contour plots of u velocity at slack water before flood tide at t = 37.26 hours. The parameters are the same as in Figure 1 except with a mixed layer of thickness (a) 50 m and (b) 150 m. The contour interval is 0.05 m/s in (a) and 0.02 m/s in (b).

solitary wave generation. The stratification in the top 300 m of the water column is replaced by a diffused thermocline with constant buoyancy frequency N = 0.015 rad/s. The result (not shown) contains only linear hydrostatic internal waves propagating away from the ridge, pointing out the need of a sharp thermocline to trap the energy in the wave beam to generate internal solitary waves. We conclude that a shallow upper-ocean mixed layer does not affect the formation of internal solitary waves, but a deep mixed layer that eliminates the sharp thermocline prevents the formation of nonlinear waves. A sharp thermocline acts as a wave guide to focus the energy in the internal wave beam. Without a strong shallow thermocline, only linear internal waves propagate away from the ridge.

IMPACT/APPLICATIONS

It seems that both lee waves and internal tides are involved in the generation of internal solitary waves. In the classical mountain wave theory, lee waves behind a mountain are upward propagating internal waves. The development of wave beams at the ridge top is similar to the generation of lee waves behind a mountain. In the meantime, horizontally propagating internal tides are produced by energy trapping in the thermocline. Large-amplitude internal tides are produced if the thermocline is sharp, and nonlinear intensification in the internal tides leads to the formation of tidal bores and solitary waves.

The Kuroshio path east of the Luzon Strait may follow a meandering loop into the South China Sea. Dr. D.-S. Ko has provided us with the monthly buoyancy frequency distribution in the vicinity of the Luzon Strait from the data base of Naval Research Laboratory at NASA's Stennis Space Center. At 400 m, the stratification over the ridges in the Luzon Strait is stronger from March to August than in the rest of the year. The change in stratification is likely associated with the seasonal migration of the Kuroshio axis. According to our numerical result, spring and summer should be the favorite period for the generation of internal wave beams.

Internal solitary waves are more likely to form when a strong shallow thermocline exists. From the monthly distribution of the depth of the isothermal surface (Qu et al., 2007, see their Figure 10), the

mixed layer depth decreases from January to June and then increases to maximum in November in the region west of Luzon Strait. The shallowest mixed layer occurs from April to August, a favorite period for formation of internal solitary waves as predicted by the present study.

RELATED PROJECTS

The wave generation hypothesis can be tested in observations. Steep-sided ridges and strong stratification near the ridge top favor the generation of internal solitary waves. We are using Steve Ramp's mooring observations on top of the ridge in the Luzon Strait to verify our hypothesis. We are also collaborating with Dong-Shan Ko to look into the generation mechanism based on climatology in the Luzon Strait. We have also worked with NLIWI participants from Taiwan (S. Jan and C.-R. Wu) on the circulation in the South China Sea, Taiwan Strait and Kuroshio.

REFERENCES

Akylas, T. R., R. H.. J.Grimshaw, S. R. Clarke, and A. Tabaei (2007) Reflecting tidal wave beams and local generation of solitary waves in the ocean thermocline, J. Fluid Mech. 593, 297-313.

Gerkema, T. (2001), Internal and interfacial tides: beam scattering and local generation of solitary waves, solitary waves, J. Mar. Res., 59, 227-255.

Qu, T., Y. Du, J. Gan, and D. Wang (2007), Mean seasonal cycle of isothermal depth in the South China Sea, J. Geophys. Res., 112, C02020, doi:10.102

Shaw, P.-T., and S.-Y. Chao (2006), A nonhydrostatic primitive-equation model for studying small-scale processes: an object oriented approach, Continental Shelf Res., 26, 1416-1432.

P.-T. Shaw, D.-S. Ko and S.-Y. Chao (2008) Internal solitary waves induced by flow over a ridge: with applications to the northern South China Sea, Journal of Geophysical Research.

PUBLICATIONS

S.-Y. Chao, D.-S. Ko, R.-C. Lien and P.-T. Shaw (2007) Assessing the west ridge of Luzon Strait as an internal wave mediator, Journal of Oceanography, vol. 63, pp. 897 to 911 [published, refereed]

Y.-C. Hsin, C.-R. Wu, and P.-T. Shaw (2008) Spatial and temporal variations of the Kuroshio east of Taiwan, 1982-2005: A numerical study, Journal of Geophysical Research, vol. 113, C04002, doi:10.1029/2007JC004485. [published, refereed]

P.-T. Shaw, D.-S. Ko and S.-Y. Chao (2008) Internal solitary waves induced by flow over a ridge: with applications to the northern South China Sea, Journal of Geophysical Research. [submitted, refereed]

C.-R. Wu, S. Y. Chao and C. Hsu (2007) Transient, seasonal and variability of the Taiwan Strait Current, Journal of Oceanography, vol. 63, pp. 821 to 883 [published, refereed]

S. Jan, C.-S. Chern, J. Wang and S. Y. Chao (2007) Generation of diurnal K_1 internal tide in the Luzon Strait and its influence on surface tide in the South China Sea, Journal of Geophysical Research, vol. 112, C06019, doi:10.1029/2006JC004003 [published, refereed]

T.-L. Chiang, C.-R. Wu and S. Y. Chao (2008). Physical and geographical origins of the South China Sea Warm Current, Journal of Geophysical Research, vol. 113, C08028, doi:10.1029/2008JC004794 [published, refereed]

C.-R. Wu, H.-F. Lu and S. Y. Chao (2008). A numerical study on the formation of upwelling off northeast Taiwan, Journal of Geophysical Research, vol. 113, C08025, doi:10.1029/2007JC004697 [published, refereed]